



**HAL**  
open science

# Rotating shear-driven turbulent flows: Towards a spectral model with angle-dependent linear interactions.

Ying Zhu, Claude Cambon, Fabien Godeferd

## ► To cite this version:

Ying Zhu, Claude Cambon, Fabien Godeferd. Rotating shear-driven turbulent flows: Towards a spectral model with angle-dependent linear interactions.. CFM 2017 - 23ème Congrès Français de Mécanique, Aug 2017, Lille, France. hal-03465685

**HAL Id: hal-03465685**

**<https://hal.science/hal-03465685>**

Submitted on 3 Dec 2021

**HAL** is a multi-disciplinary open access archive for the deposit and dissemination of scientific research documents, whether they are published or not. The documents may come from teaching and research institutions in France or abroad, or from public or private research centers.

L'archive ouverte pluridisciplinaire **HAL**, est destinée au dépôt et à la diffusion de documents scientifiques de niveau recherche, publiés ou non, émanant des établissements d'enseignement et de recherche français ou étrangers, des laboratoires publics ou privés.

# Rotating shear-driven turbulent flows : Towards a spectral model with angle-dependent linear interactions

Y. ZHU, C. CAMBON, F. S. GODEFERD

Laboratoire de Mécanique des Fluides et d'Acoustique  
UMR 5509, CNRS, Université de Lyon,  
ECL, UCBL, INSA — Lyon, France.  
claude.cambon@ec-lyon.fr

## Résumé :

*Nous présentons un nouveau modèle statistique pour la turbulence homogène soumise à des distorsions. Ce modèle améliore et prolonge celui de Mons et al. (MCS). Il prend en compte sans modélisation et sans troncature les termes linéaires dans les équations pour le spectre d'énergie  $\mathcal{E}(\mathbf{k}, t)$  et le déviateur de polarisation  $Z(\mathbf{k}, t)$ , qui engendrent le tenseur spectral des corrélations doubles de vitesse en turbulence homogène arbitrairement anisotrope, en présence de gradients de vitesse moyenne et de rotation d'ensemble. Seuls les termes de transfert, qui reflètent l'impact dans ces équations des corrélations triples en deux points, gardent la formulation anisotrope MCS simplifiée à partir d'EDQNM (Eddy Damped Quasi-Normal Markovian), via une troncature au premier ordre significatif en harmoniques angulaires. Le nouveau modèle numérique est validé sur les termes qui reproduisent la limite de distorsion rapide (RDT) non visqueuse, pour le cisaillement tournant, et comparé aux résultats de RDT de Salhi et al. (2014). L'accord est excellent pour différents rapports de vortacité  $R = 2\Omega/(-S)$ , où  $\Omega$  est la vitesse angulaire du repère tournant et  $S$  le taux de cisaillement, avec notre schéma numérique qui est très différent de la méthode des caractéristiques utilisée en RDT et en simulation numérique directe. Ces comparaisons montrent en outre que le modèle MCS n'est valide que jusqu'à des valeurs faibles de  $St$  dans cette limite linéaire. Cette validation sur la dynamique linéaire est une étape cruciale pour notre future étude non-linéaire multi-échelles, car cette dynamique est toujours très significative dans le domaine infrarouge des spectres d'énergie, même quand elle est globalement marginale dans l'évolution des grandeurs statistiques en un point.*

## Abstract :

*We propose a new statistical model for homogeneous turbulence undergoing distortions, which improves and extends the MCS model by Mons et al. (2016). The spectral tensor of double velocity correlations is predicted in the presence of arbitrary mean velocity gradients, and in a rotating frame. For this, we numerically solve coupled equations for the angle-dependent energy spectrum  $\mathcal{E}(\mathbf{k}, t)$ , that includes directional anisotropy, and the deviatoric pseudo-scalar  $Z(\mathbf{k}, t)$ , that underlies polarization anisotropy. These equations include two parts : (1) exact linear terms representing the viscous RDT (Rapid Distortion Theory) solution when considered alone ; (2) generalized transfer terms mediated by two-point*

third-order correlations. The latter are closed by an EDQNM (Eddy Damped Quasi-Normal Markovian) anisotropic technique. Using a truncated expansion in terms of angular harmonics, we express the spherically-averaged descriptors of the transfer terms in terms of the corresponding descriptors of the second-order spectral tensor, as done in MCS. However, in contrast with MCS, the complete angular dependence is kept for solving the linear terms. A first validation of the new ‘linear RDT solver’ is performed with respect to RDT and DNS of rotating shear flow (Salhi et al. 2014, in which a characteristics technique is used). Results accurately compare in the inviscid RDT limit for typical stabilizing and destabilizing cases related to various ratios  $R$  of system vorticity  $2\Omega$  to shear-induced vorticity  $-S$ . Comparisons also confirm that MCS is limited to small values of  $St$  in this linear limit. This paves the way for a fully nonlinear scale-by-scale and anisotropic study, in which RDT is never globally dominant for single-point statistics, but is crucial for predicting the largest scales and the infrared range.

**Mots clefs : Turbulence, cisaillement tournant, modèle multi-échelle**

## 1 Introduction

The interplay between linear and nonlinear mechanisms can be very complex and subtle in turbulent shear flows. Rapid Distortion Theory (RDT) of homogeneous turbulence is very powerful for solving linear operators induced by rotational mean flows [1], but its relevance is limited in principle to short evolution times, and more specifically to the largest scales of the turbulent flow if a scale-by-scale approach is performed.

Among various combinations of mean strain and mean vorticity, the case of mean plane shear rotating in the spanwise direction has various applications in engineering, geophysics and astrophysics. Stabilizing and destabilizing effects of the system vorticity are found in rotating plane channel flows, with experimental study [2] and simple modelling [3, 4] also valid in atmospheric flows. The homogeneous rotating shear flow is also a model for turbulent accretion discs in astrophysics, according to the Sheared Sheet Approximation (SSA) by [5]. Normal mode stability is governed by the Bradshaw number, or  $B = R(R + 1)$ , in which  $R = -2\Omega/S$  is the ratio of system vorticity  $2\Omega$  to shear-induced-vorticity  $-S$ , with  $S$  the shear rate. As confirmed by RDT,  $B < 0$  or  $-1 < R < 0$  corresponds to exponential growth, and  $B > 0$  to exponential decay. Neutral cases are found for both  $R = 0$  (no additional rotation) and  $R = -1$  (zero absolute vorticity).

Fully nonlinear DNS were performed by [6] without scale-by-scale analysis, and by [7] for a spectral analysis. To which extent such DNS results can be used for validating a statistical spectral model, that could extrapolate them towards very high Reynolds number? On the one hand, this strategy—validation versus DNS continued by extrapolation—was successful for buoyancy-driven flows, using a generalized anisotropic EDQNM (Eddy Damped Quasi-Normal Markovian [9]) model for unstable stratification [8]. On the other hand, the model recently validated for shear-driven flow by [10] (MCS for Mons, Cambon & Sagaut hereinafter) ought to be improved for quantitative and accurate comparisons with DNS : It is expected that nonlinear mechanisms for energy transfer and return-to-isotropy are satisfactory, but not the linear mechanisms related to RDT when they are dominant. An improved model is in construction, and this article gives its first validation in the RDT limit for the rotating shear.

In the following, Section 2 presents basic equations and numerical challenges. Preliminary numerical results are given and discussed in Section 3. Section 4 is devoted to conclusions and perspectives.

## 2 Basic equations and numerical approach

Following Batchelor and Craya, we consider the general case of statistical homogeneity restricted to fluctuations, in which an extensional mean flow  $U_i$  injects energy and anisotropy into the fluctuating flow via spatially uniform mean velocity gradients  $A_{ij}$  :

$$A_{ij} = \frac{\partial U_i}{\partial x_j} = S_{ij} + \frac{1}{2} \epsilon_{imj} W_m, \quad (1)$$

combining contributions from strain  $S_{ij}$ , its symmetric part, and mean vorticity  $\mathbf{W}$ , that generates its antisymmetric part. In addition, the whole flow—mean + fluctuating—can be seen in a rotating frame with angular velocity  $\mathbf{\Omega}$  for various applications, such as rotating shear or precessing flows.

Looking at the fluctuating velocity field  $u_i$ , the most general information on two-point second-order velocity correlations is given by the tensor  $R_{ij}(\mathbf{r}) = \langle u_i(\mathbf{x})u_j(\mathbf{x} + \mathbf{r}) \rangle$ , and the related spectral tensor  $\hat{R}_{ij}(\mathbf{k})$  obtained by three-dimensional Fourier transform. In this context, our *basic state vector* for representing two-point second-order correlations is the set  $(\mathcal{E}, Z)$ , which generates the spectral tensor  $\hat{R}_{ij}(\mathbf{k})$  with all its components but the helicity spectrum (see [7]) :

$$\hat{R}_{ij}(\mathbf{k}, t) = \mathcal{E}(\mathbf{k}, t) (\delta_{ij} - \alpha_i \alpha_j) + \Re(Z(\mathbf{k}, t) N_i(\boldsymbol{\alpha}) N_j(\boldsymbol{\alpha})). \quad (2)$$

The set  $(\mathbf{N}, \mathbf{N}^*, \boldsymbol{\alpha})$  generates an orthonormal frame for projecting the velocity field in Fourier space  $\hat{\mathbf{u}}(\mathbf{k}, t)$ , and is closely related to the Craya-Herring frame of reference [13].  $\mathbf{N}$  and its conjugate  $\mathbf{N}^*$  are the helical modes [14]

$$\mathbf{N}(\boldsymbol{\alpha}) = \mathbf{e}^{(2)}(\boldsymbol{\alpha}) - i\mathbf{e}^{(1)}(\boldsymbol{\alpha}), \quad \boldsymbol{\alpha} = \frac{\mathbf{k}}{|\mathbf{k}|}, \quad \mathbf{e}^{(1)}(\boldsymbol{\alpha}) = \frac{\boldsymbol{\alpha} \times \mathbf{n}}{|\boldsymbol{\alpha} \times \mathbf{n}|}, \quad \mathbf{e}^{(2)}(\boldsymbol{\alpha}) = \boldsymbol{\alpha} \times \mathbf{e}^{(1)}(\boldsymbol{\alpha}), \quad (3)$$

in which  $\mathbf{k}$  is the three-dimensional wavevector, seen in a system of polar-spherical coordinates of polar axis  $\mathbf{n}$ , and  $i^2 = -1$ .

Equations for the state vector  $(\mathcal{E}, Z)$  are derived from the equation for the divergence-free fluctuating field, in which the pressure fluctuation is solved and thereby removed from consideration, so that

$$(\dot{k}\mathcal{E}) + 2\nu k^3 \mathcal{E} + \Re(kZ(\mathbf{k}, t) S_{ij} N_i(\boldsymbol{\alpha}) N_j(\boldsymbol{\alpha})) = kT^{(\mathcal{E})}(\mathbf{k}, t) \quad (4)$$

and

$$(\dot{k}Z) + 2\nu k^3 Z + k\mathcal{E}(\mathbf{k}, t) S_{ij} N_i(-\boldsymbol{\alpha}) N_j(-\boldsymbol{\alpha}) - ikZ(\mathbf{k}, t) ((\mathbf{W} + 4\boldsymbol{\Omega}) \cdot \boldsymbol{\alpha} - 2\Omega_E) = kT^{(Z)}(\mathbf{k}, t), \quad (5)$$

in which  $\nu$  is the kinematic viscosity. The overdot corresponds to the advection operator due to the presence of mean flow :

$$(\dot{\dots}) = \frac{\partial}{\partial t} - A_{mn} k_m \frac{\partial}{\partial k_n}. \quad (6)$$

The left-hand-sides of both equations (4) and (5) reflect the linear effects of the mean flow, as in viscous Rapid Distortion Theory, with geometric coefficients that depend on the orientation of the wave vector  $\boldsymbol{\alpha} = \mathbf{k}/k$  via helical modes  $\mathbf{N}(\pm\boldsymbol{\alpha})$ .  $\Omega_E$  is a special rotation rate induced by the advection operator, that can be removed from consideration in the special applications used in this article.

The right-hand-sides of both equations gather the contribution from two-point third-order correlations

mediated by the quadratic nonlinearity of basic Navier-Stokes equations.

## 2.1 Closure of generalized nonlinear transfer terms

The closure of the generalized transfer terms  $T^{(\mathcal{E})}$  and  $T^{(Z)}$  in terms of  $\mathcal{E}$  and  $Z$  is performed via an anisotropic EDQNM procedure, called EDQNM1, used and revisited in [10] and in [15]. Faced with the high computational cost of solving these equations for all wavevector directions, a second step was applied to restrict the description to spherically averaged descriptors. This purely technical step amounts to replacing fully anisotropic  $\mathcal{E}$  and  $Z$  terms by the truncated expansions

$$\mathcal{E}(\mathbf{k}, t) = \frac{E(k, t)}{4\pi k^2} \left( 1 - 15H_{mn}^{(dir)}(k, t)\alpha_m\alpha_n \right) \quad (7)$$

and

$$Z(\mathbf{k}, t) = \frac{5}{2} \frac{E(k, t)}{4\pi k^2} H_{mn}^{(pol)}(k, t) N_m^*(\boldsymbol{\alpha}) N_n^*(\boldsymbol{\alpha}). \quad (8)$$

These expansions involve the non-dimensional deviatoric tensors  $H_{mn}^{(dir)}$  and  $H_{mn}^{(pol)}$  which are given by integrating  $\hat{R}_{ij}(\mathbf{k}, t)$  on spherical shells of radius  $k = |\mathbf{k}|$ , so that

$$\varphi_{ij}(k, t) = \int_{S_k} \hat{R}_{ij}(\mathbf{k}, t) d^2\mathbf{k} = 2E(k, t) \left( \frac{1}{3}\delta_{ij} + H_{ij}^{(dir)}(k, t) + H_{ij}^{(pol)}(k, t) \right). \quad (9)$$

The three contributions, isotropic, directional anisotropy and polarization anisotropy derive, term-to-term from Eq. (2), in which  $\mathcal{E}(\mathbf{k}) = \frac{E(k)}{4\pi k^2} + \mathcal{E}^{(dir)}(\mathbf{k})$ , with  $E(k)$  the classical spherically-integrated energy spectrum, only present in isotropic turbulence. On the one hand, it is possible to extract from an arbitrary anisotropic spectral tensor  $\hat{R}_{ij}$  the set of spherically-averaged descriptors  $(E, H_{ij}^{(dir)}, H_{ij}^{(pol)})$ , in which directional anisotropy and polarization anisotropy are disentangled. On the other hand, it is possible to reconstruct a part of the full spectral tensor by means of these descriptors using Eqs. (7) and (8).

It is consistent to express the generalized transfer terms using the same truncated expansion, or

$$T^{(\mathcal{E})}(\mathbf{k}, t) = \frac{T(k, t)}{4\pi k^2} \left( 1 - 15\tilde{S}_{mn}^{NL(dir)}(k, t)\alpha_m\alpha_n \right) \quad (10)$$

and

$$T^{(Z)}(\mathbf{k}, t) = \frac{5}{2} \frac{T(k, t)}{4\pi k^2} \tilde{S}_{mn}^{NL(pol)}(k, t) N_m^*(\boldsymbol{\alpha}) N_n^*(\boldsymbol{\alpha}). \quad (11)$$

A closed system of equations is derived in MCS for the set  $(E, H_{ij}^{(dir)}, H_{ij}^{(pol)})$ , in which linear terms in the left-hand-side of Eqs. (4) and (5) give contributions  $T^L, S_{ij}^{L(dir)}$  and  $S_{ij}^{L(pol)}$ , whereas nonlinear contributions yield the above-mentioned  $T, \frac{T}{4\pi k^2} \tilde{S}_{ij}^{NL(dir)}$  and  $\frac{T}{4\pi k^2} \tilde{S}_{ij}^{NL(pol)}$  terms. In short, a model using only spherically-averaged descriptors is exactly derived from the EDQNM1 model in  $\mathbf{k}$ -vector space, using second-order truncated expansions just described.

The resulting simplified model MCS is flexible, versatile, and tractable. Its nonlinear part reduces to calculations similar to those of isotropic EDQNM, and it has been validated for several flow cases, including effects of irrotational straining processes ( $A_{ij}$  symmetric, possibly time-dependent), plane shear, and return-to-isotropy when mean flow gradients are removed. On the other hand, the rapid distortion limit is no longer exact in the MCS model, because the very strong anisotropy induced by RDT requires higher order angular harmonics than the mere degree 2 in Eqs. (7) and (8). Accordingly, preliminary

comparisons between DNS and MCS model are not satisfactory for the largest scales, or smallest wavenumbers, in which full RDT, that possibly compete with nonlinear backscatter, ought to be captured with care.

## 2.2 Numerical procedure, with mean flow advection

The first goal of this study is to numerically solve the system of Eqs. (4) and (5) for various mean flow gradients, with controlled accuracy for the linear terms and generalized transfer terms given by Eqs. (10) and (11), still using their spherically averaged descriptors closed by the MCS model.

The main difficulty is to solve the advection operator (6). In theoretical RDT, as well as in fully nonlinear DNS by [11] and [12], the scheme amounts to following  $(\mathbf{k}, t)$  characteristic lines, connected with mean trajectories in physical space, so that the wave vector is rendered time-dependent with  $\dot{\Phi}(\mathbf{k}(t), t) = \frac{\partial \Phi}{\partial t} + \frac{\partial \Phi}{\partial k_m} \frac{dk_m}{dt}$ . A different procedure is chosen here : A finite-difference scheme is used for expressing the  $\frac{\partial}{\partial k_n}$ -derivatives, with discretization of the wave-vector consistent with a system of polar-spherical coordinates. With respect to the method of characteristics, there is no need for interpolation, or ‘reme-shing’, from  $\mathbf{k}(t)$ -space to  $\mathbf{k}(t_0)$ -space, and the orientation of the wave vector can be discretized with high accuracy in Fourier space ; as in EDQNM calculations and shell-models, a logarithmic step is very convenient for the modulus of the wave number. This numerical procedure is well suited for the  $(\mathbf{k}, t)$  development of smooth statistical quantities, although it should be questionable in Rogallo’s pseudo-spectral DNS, started with randomly initialized velocity modes.

In practice, the finite differences scheme (FDS) we use for discretizing derivatives with respect to  $k_m$  in the advection term is a sixth-order explicit centered scheme. We have tested accuracy with respect to the order of the spatial scheme, using different FDS : centered FDS from second- to eighth-order ; upwind FDS from second- to fifth-order ; Lax-Wendroff FDS. The results of these tests show that enough accuracy for the sheared turbulence case is obtained only starting with sixth-order centered FDS. The strongest accuracy constraint for computing  $\partial/\partial k_m$  is in the small-scale range (large wavenumbers), due to the sparse mesh elements distribution there.

Time-marching uses a fourth-order Runge-Kutta scheme, which is perfectly adequate for high accuracy and sufficient stability.

## 3 Application to plane shear rotating in the spanwise direction

The mean plane shear is characterized by  $A_{ij} = S\delta_{i1}\delta_{j2}$ , the indices 1, 2 and 3 referring to streamwise, cross-gradient, and spanwise directions, respectively. In our first application, as in [7], the additional system vorticity  $2\Omega$  is chosen in the spanwise direction.

### 3.1 Validation and results for linear inviscid dynamics

The inviscid RDT limit is very subtle to capture because, even looking at the left-hand-sides of Eqs. (4) and (5), with zero right-hand sides, local angle-dependent terms in Fourier space coexist with the nonlocal advection operator (6), that induces a linear transfer in wavespace.

Without additional system vorticity, the MCS model is already disappointing in this limit. The algebraic growth of kinetic energy is missed, and exponential growth is predicted instead, as shown on Fig. 1-left. Looking at the energy spectrum (Fig. 1-right), initialized as in MCS, it is confirmed that spectral energy is largely overestimated in MCS at almost all scales, except the smallest ones.

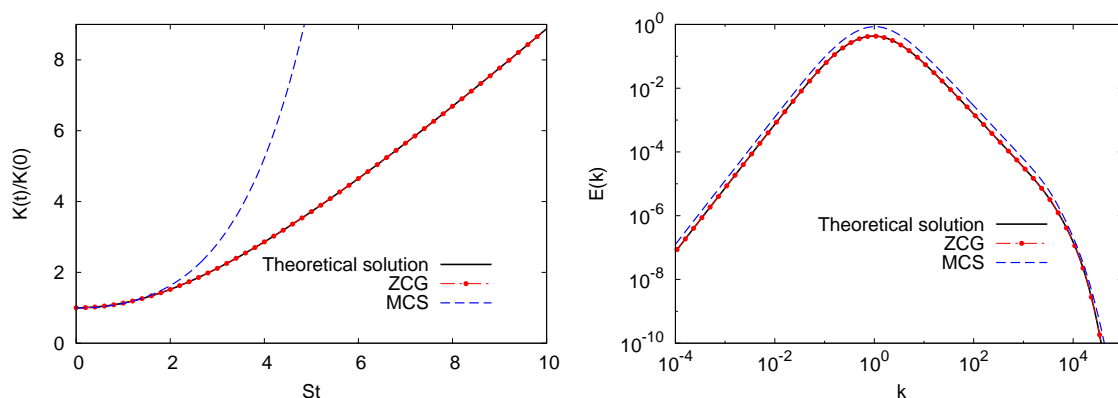


FIGURE 1 – Inviscid RDT limit,  $R = 0$ . Left : time-evolution of kinetic energy from both present (ZCG) model and MCS model. Right : Corresponding energy spectra at  $St = 4$ .

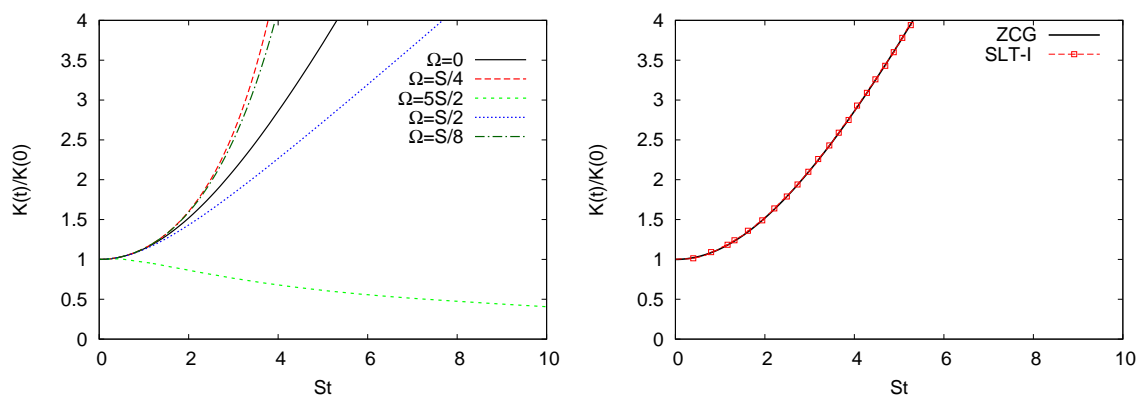


FIGURE 2 – Left : time-evolution of kinetic energy for various  $R = 2\Omega/(-S)$ -ratios, present model. Right : comparison of results from the present model with those of [7],  $R = 0$ .

However, as shown by the two plots of Figure 1, the exact theoretical solution for time-evolution of kinetic energy and the spectral distribution, is accurately reproduced by our present model (which we call ZCG), with and without additional rotation.

In Figure 2, typical cases, with different combinations of strain and rotation, are plotted :  $R = -5$  (or  $\Omega = 5S/2$ , stabilizing, anticyclonic case),  $R = -1$  (or  $\Omega = S/2$ , neutral, zero absolute vorticity, as in the central region of a rotating channel),  $R = -1/2$  (or  $\Omega = S/4$ , maximum destabilization, anticyclonic case, as in the pressure side), and  $R = 0$  (no rotation). Our ZCG model's predictions agree very well with the results in [7], obtained in the same limit (inviscid RDT) by a different characteristics technique. The comparison is plotted only for  $R = 0$  in Fig. 2-right, for the sake of brevity. The case  $R = -1/4$  in Fig. 2, not addressed in [7] appears close to maximum destabilization.

## 4 Conclusions and perspectives

A model that improves the MCS one—at least regarding the treatment of linear operators due to distortions of the flow—has been constructed and validated in the inviscid RDT limit for the rotating shear flow. In conventional single-point modeling, the accurate capture of RDT is not possible, and only coarse approximations are offered. In practical flow cases, however, the linear, or ‘rapid’, terms are not dominant, as reflected by a moderate value of the typical shear-rapidity term, as  $SK/\varepsilon$ , or ratio of shear rate to turnover time scale, *e.g.* the dissipation rate over the kinetic energy.

However, RDT, possibly competing with backscatter, cannot be considered as a side effect, even at large elapsed time, if we want to predict all the scales, in a true scale-by-scale approach. The related challenge of predicting the largest scales of turbulence, including the infrared range, is illustrated by [8] in buoyancy-driven flows. In addition, the RDT operators are much more puzzling in the shear-driven flow case than in [8], because of the presence of the *mean-flow-advection operator* (see also [15].) Accordingly, we think that the challenge of reproducing RDT is difficult, so that this first validation of a future accurate model including both linear and non linear terms, is an important milestone towards a fully nonlinear anisotropic spectral model.

All the equations are given and implemented in a numerical code for this purpose, so that we can expect a useful compromise between an efficient RDT-solver and the relevant nonlinear structure inherited from the MCS model. Validation in the nonlinear cases addressed in [7] is the next future step.

Note that our model can be consistently linked to single-point models that are for instance constructed on advanced rationale, such as the structure-based modelling [16], recently revisited by [17].

## Références

- [1] K. H. Moffatt, Interaction of turbulence with strong wind shear, in Colloquium on Atmospheric Turbulence and Radio Wave Propagation, edited by A. M. Yaglom and V. I. Tatarski, Nauka, Moscow (1967) 139–156.
- [2] J. P. Johnson, R. M. Halleen, D. K. Lezius, Effects of spanwise rotation on the structure of two-dimensional fully developed turbulent channel flow, *J. Fluid Mech.* **56**, 3 (1972) 533–557.
- [3] P. Bradshaw, The analogy between streamline curvature and buoyancy in turbulent shear flow, *J. Fluid Mech.* **36** (1969) 177–191.
- [4] D. J. Tritton, Stabilization and destabilization of turbulent shear flow in a rotating fluid, *J. Fluid Mech.* **241** (1992) 503–523.
- [5] S. A. Balbus, J. F. Hawley, Instability, turbulence, and enhanced transport in accretion discs, *Rev. Mod. Phys.* **70** (1998) 1.
- [6] G. Brethouwer, The effect of rotation on rapidly sheared homogeneous turbulence and passive scalar transport. Linear theory and direct numerical simulation, *J. Fluid Mech.* **542** (2005) 305–342.
- [7] A. Salhi, F. Jacobitz, K. Schneider, C. Cambon, Nonlinear dynamics and anisotropic structure of rotating sheared turbulence, *Phys. Rev. E*, **89** (2014) 013020.
- [8] A. Burlot, B.-J. Gréa, F. S. Godeferd, C. Cambon, O. Soulard, Large Reynolds number self-similar states of unstably stratified turbulence, *Phys. Fluids* **27** (2015) 065214.
- [9] S. A. Orszag, Analytical theories of turbulence, *J. Fluid Mech.* **41**, 2 (1970) 363–386.
- [10] V. Mons, C. Cambon, P. Sagaut, A spectral model for homogeneous shear-driven turbulence in terms of spherically-averaged descriptors, *J. Fluid Mech.* **788** (2016) 147–182.
- [11] R. S. Rogallo, NASA TM 81315 (1981)
- [12] G. Lesur, from 2005 : his *Snoopy* code is very popular among astrophysicists and is available online.
- [13] J. R. Herring, Approach of axisymmetric turbulence to isotropy, *Phys. Fluids* **17** (5) (1974) 859–872.
- [14] C. Cambon, L. Jacquin, Spectral approach to non-isotropic turbulence subjected to rotation, *J. Fluid Mech.* **202** (1989) 295–317.

- 
- [15] C. Cambon, V. Mons, B. -J. Gréa, R. Rubinstein, Anisotropic triadic closures for shear-driven and buoyancy-driven turbulent flows, *Computers and Fluids* (2016).
- [16] S. Kassinos, W. C. Reynolds, M. M. Rogers, One-point turbulence structure tensors, *J. Fluid Mech.* **428** (2001) 213–248.
- [17] A. A. Mishra, S. S. Girimaji, Towards approximating non-local dynamics in single-point pressure strain correlation closures, *J. Fluid Mech.* **811** (2017) 168–188.